Giant Intracranial Aneurysms at 7 Tesla MRI: A New Diagnostic Approach to Understand This Rare Intracranial Vascular Pathology

Bixia Chen[1,2], Toshinori Matsushige[2,3], Stefan Maderwald[1], Sören Johst[1], Harald H. Quick[1,4], Mark Edward Ladd[1,5], Ulrich Sure[2], and Karsten Henning Wrede[1,2]
[1]Erwin L. Hahn Institute for Magnetic Resonance Imaging, University Duisburg-Essen, Essen, NRW, Germany, [2]Department of Neurosurgery, University Hospital Essen, University Duisburg-Essen, Essen, NRW, Germany, [3]Department of Neurosurgery, Hiroshima University Hospital, Hiroshima University, Hiroshima, Hiroshima Prefecture, Japan, [4]High Field and Hybrid MR Imaging, University Hospital Essen, University Duisburg-Essen, Essen, NRW, Germany, [5]Medical Physics in Radiology, German Cancer Research Center (DKFZ), Heidelberg, BW, Germany

Target Audience: Researchers working on neurovascular imaging / ultra-high-field MRI.

Introduction:

Giant intracranial aneurysms (IGA) (size > 25 mm) are rare vascular lesions with a high rupture risk[1]. Subarachnoid hemorrhages from ruptured aneurysms are associated with high morbidity and mortality. Inflammatory processes and intraluminal thromboses are believed to be related to wall degeneration and aneurysm rupture[2]. This study aims to characterize giant intracranial aneurysms with focus on aneurysm wall properties and thickness at 7 Tesla (T) magnetic resonance imaging (MRI).

Material and Methods:

Six patients with giant intracranial aneurysms were prospectively evaluated using a 7T whole-body MR system (Magnetom 7T, Siemens) with a 32-channel head coil (Nova Medical, Wilmington, USA) from April 2011 to October 2014. All unruptured giant aneurysms were previously diagnosed using conventional MRI (1.5T or 3T) and DSA. Three patients were male, the average age in the collective was 65.2 years (range 50-80 years). Three aneurysms were located at the middle cerebral artery (MCA), two at the internal carotid artery (ICA), and one at the basilar artery (BA). The applied modified sequences at 7T included time-of-flight (TOF)[3], magnetization-prepared rapid acquisition gradient-echo (MPRAGE)[4], and susceptibility weighted imaging (SWI). The sequence with the highest spatial resolution was TOF featuring an image resolution of 0.22 x 0.22 x 0.41 mm^3. The region of interest (ROI) was placed in the wall of the dome farthest away from the aneurysm base. Two raters assessed aneurysm and parent artery (PA) diameter (diam), wall thickness, signal intensity of aneurysm wall, intraluminal thrombus, intraluminal flow, and surrounding brain tissue in consensus reading. In addition, the contrast ratios of the aneurysm wall to adjacent brain parenchyma, intraluminal thrombus, and intraluminal flow were calculated. Two surgically resected aneurysms were suitable for histological examination, and correlation between MRI and histopathology was evaluated.

Results:

Imaging studies revealed two completely thrombosed aneurysms, three partially thrombosed aneurysms, and one aneurysm without intraluminal thrombus. Major anatomical features of all aneurysms are summarized in Table 1. Both patients with completely thrombosed aneurysms were conservatively observed. Two patients underwent operative clipping and resection and two patients were treated interventionally by coil embolization or parent vessel occlusion. The mean diameters of aneurysm and parent artery were 30.1 mm and 3.0 mm. The wall showed low signal intensity on TOF and SWI, with variation in signal intensity on MPRAGE. In one patient with an aneurysm of the cavernous part of the ICA, evaluation of SWI was excluded because of major susceptibility artifacts near the skull base. The mean contrast ratio to surrounding brain parenchyma on TOF, magnitude SWI, and SWI were -0.42± 0.22, -0.69± 0.08, and -0.87± 0.08, respectively. The mean and SD of the aneurysm wall thickness was 0.942± 0.289 mm in the TOF sequence, 1.082± 0.328 mm in MPRAGE, 1.355± 0.179 mm in magnitude SWI, and 1.497± 0.219 mm in (MIP-)SWI. In TOF and SWI (Figure 1), the aneurysm wall was depicted triple-layered with a hyperintense signal in the middle layer. In two available histopathological specimens, the hyperintense layer was identical to the tunica media. There was no iron deposition within this part of the wall in the Prussian blue stain, while tunica externa and tunica intima had strong iron uptake. The actual wall thickness corresponded best to the measured wall thickness in the TOF sequence for both patients who were operated upon.

No.	Age (years)	Sex	Location	Thrombosis	Max. aneurysm diam (mm)	Aneurysm neck diam (mm)	PA diam (mm)
1	50	f	ICA	partially	25.06	4.38	3.85
2	56	f	ICA (cavernous)	none	37.87	7.95	3.43
3	75	m	MCA	partially	35.78	6.79	3.04
4	80	m	MCA	completely	28.99	7.31	1.70
5	61	f	MCA	partially	25.95	5.60	2.46
6	69	m	BA	completely	27.21	22.10	3.57

Table 1: *Patient demographics and anatomical characteristics of aneurysms*

Discussion and Conclusion:

In 7T MRI, the walls of intracranial giant aneurysms were well depicted with low signal intensity in TOF and SWI sequences compared to adjacent tissue structures. 7T TOF and SWI could precisely reveal microstructures in the aneurysm wall as seen in histopathology. The grade of iron deposition in individual wall layers, supposed to be related to inflammation, was depictable and might serve as a future follow-up marker. The valuable information gained from wall imaging in this small case series warrants further studies with larger patient cohorts. Ultra-high-field MRI of this rare intracranial vascular pathology might contribute to a better understanding of the complex pathophysiology of aneurysm growth and rupture.

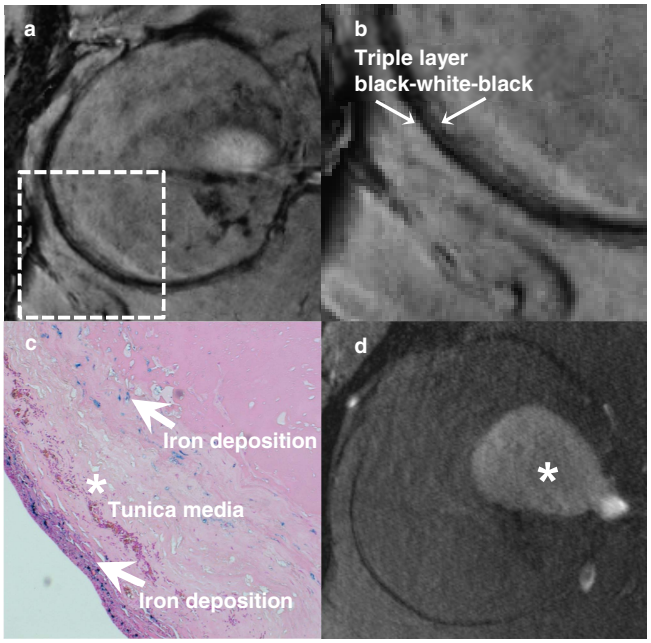

Figure 1: *(a) Intracranial giant aneurysm on (MIP-)SWI sequence at 7T. (b) Triple-layered aneurysm wall in the magnified SWI image. (c) Histopathology (Prussian blue): Absence of iron staining in the tunica media. (d) Intraluminal flow (*) in the partially thrombosed giant aneurysm on TOF sequence.*

References: 1. Gross et al. J Clin Neurosci. 2013;20(6):776-82. 2. Turjman et al. Circulation. 2014;129(3):373-82. 3. Johst et al. Invest Radiol. 2012;47(8):445-50. 4. Wrede et al. Acad Radiol. 2012;19(2):172-8.

The research leading to these results has received funding from the Interne Forschungsförderung Essen (IFORES), University Hospital Essen, University Duisburg-Essen.